EFFECT OF SOOT FORMATION ON DROPLET COMBUSTION

Fernando F. Fachini

fachini@lcp.inpe.br

Instituto Nacional de Pesquisas Espaciais - INPE

Rod. Presidente Dutra km 40, 12630-000, Cachoeira Paulista- SP - Brazil

Abstract. *This work addresses the influence of the soot formation on the properties of the droplet combustion. To gain insight of the problem, the soot formation model is based on some simplifying assumptions: the pyrolysis reaction $Fuel \rightarrow Soot$ is considered infinitely fast. The soot formation is responsible for changing drastically the flame properties in droplet combustion. This theoretical result is in concordance to the experimental results presented in the literature. Besides the objective of soot modelling, the aim of this work is also to provide a very fast numerical tool to be used in spray combustion codes to determine the properties of an isolated droplet combustion. To achieve this goal, an extension of the Shvab-Zel'dovich formulation, that uses an integro-differential description of the excess enthalpy and mixture fraction, is presented.*

Keywords: *Shvab-Zel'dovich Formulation, Droplet Combustion, Soot Formation, Diffusion Flame*

1. INTRODUCTION

It is well known that fuels with very small stoichiometric fuel-air ratios do not burn completely and soot is formed [Faeth (1977); Nayagan et al. (1998); Avedisian (2000); Avedisian and Jackson (2000); Ueda et al. (2002); Xu et al. (2004); Manzello et al. (2004); Akerman et al. (2005)]. Heavy fuels satisfy the burning condition of very small stoichiometric fuel-air ratios. The classical theory of droplet combustion points out that heavy fuels burn completely and generate flame far from the droplet, of order of the inverse of the stoichiometric fuel-air ratio. However, experimentally this result is not observed. The reason for the discrepancy between the theoretical and experimental results is the soot formation.

Soot does affect the droplet combustion not only by the quantity of unburned fuel, but also by the soot thermal radiative energy loss and by the soot dynamic. In this analysis, these two former processes are not included in the model. After the soot particle is formed in a region high-temperature, fuel-rich region, close to the flame, the thermophoretic force pushes it in the direction of the droplet surface. A soot shell is formed around the droplet where the drag force is equal to the thermophoretic force. A detailed model describes the soot shell and is able to predict well the flame standoff distance (Kumar et al., 2002). The results confirm the strong influence on the droplet combustion properties.

However, due to high computational cost, detail model like that can not be used in spray combustion numerical analysis in order to describe the processes in scales smaller than the grid scale. A solution is to find simplified model with low computational cost but able to predict reasonably those processes. With this focus, a model was developed with leakage of unburned fuel by the flame representing soot formation (Fachini, 2005). The results revealed the dynamics of the flame but the standoff distance increases instead of decreasing. Invalidating the model to be used in description of the soot effect.

This work has the same objective of the previous one, but the model considers the soot formation by a simplified reaction and no fuel leakage by the flame.

2. MATHEMATICAL FORMULATION

Formulation and solution of quasi-steady droplet combustion are presented elsewhere (Fachini, 1999). Thus, because of the problem to be well known, only the parts of the formulation essential for the understanding will be explicitly presented.

Considering the ambient conditions to be characterised by the temperature T_∞, density ρ_∞, oxygen mass fraction $Y_{O\infty}$. Without loosing any important feature of the problem, the constant pressure specific heat is supposed constant, but the transport coefficients (thermal conductivity and diffusion coefficient, respectively) are dependent only on temperature according to $k/k_\infty = D_i/D_{i\,\infty} = (T/T)^n = \theta^n$. The nondimensional quasi-steady conservation equations, describing the gas phase around the droplet with radius a at time t (a_0 at the time $t = 0$), are expressed by

$$x^2 \varrho v = \lambda(\tau) \tag{1}$$

$$\frac{\lambda}{x^2}\frac{\partial}{\partial x}\left\{\begin{array}{c} Le_F y_F \\ Le_O y_O \\ \theta \end{array}\right\} - \frac{1}{x^2}\frac{\partial}{\partial x}\left(x^2 \theta^n \frac{\partial}{\partial x}\left\{\begin{array}{c} y_F \\ y_O \\ \theta \end{array}\right\}\right) =$$

$$\dot{\omega}_F Le_F \left\{\begin{array}{c} -1 \\ -S \\ Q \end{array}\right\} + \dot{\omega}_{so} Le_F \left\{\begin{array}{c} -1 \\ 0 \\ -Q_{so} \end{array}\right\} \tag{2}$$

The definition of the nondimensional independent variables are as following: the time $\tau \equiv t/t_c$, where t_c is the vaporisation time $t_c \equiv \varepsilon(a_0^2/\alpha_\infty)$ and the radial coordinate $x \equiv r/a_0$; $\varepsilon \equiv \rho_\infty/\rho_l$ is the ratio of the gas density to the liquid density and $\alpha_\infty \equiv k_\infty/(\rho_\infty c_p)$ is the thermal diffusivity. The definition of the nondimensional dependent variables (temperature, density, oxygen mass fraction, fuel mass fraction and velocity, respectively) are as following: $\theta \equiv T/T_\infty$, $\varrho \equiv \rho/\rho_\infty$, $y_O \equiv Y_O/Y_{O\infty}$, $y_F \equiv Y_F$ and $v \equiv Va_0/\alpha_\infty$. The parameters appearing in Eqs. (2) are defined as: Lewis number $Le_i \equiv \alpha_\infty/D_{i\,\infty}$, $S \equiv Le_O s/Le_F$ and $s \equiv \nu/Y_{O\infty}$ the quantity of air necessary to burn stoichiometrically a unit of mass of fuel $[F + \nu O_2 \rightarrow (1 + \nu)P]$, heat of combustion $Q \equiv q/(Le_F c_p T_\infty)$ and heat necessary for a unit mass of soot $Q_{so} \equiv q_{so}/(Le_F c_p T_\infty)$ to be formed. In this work, S satisfies the condition $S \gg 1$. Since the fuel oxidation kinetic mechanism is supposed to be one-step and the reaction rate follows Arrhenius type,

$$\dot{\omega}_F = \frac{Ba_0^2}{\alpha_\infty}\frac{\rho_\infty^{n_1+n_2-1}}{W_O^{n_1}W_F^{n_2}}y_O^{n_1}y_F^{n_2}exp(-\theta_a/\theta) \tag{3}$$

where W_i is the molecular weight of species i and the nondimensional activation energy is defined by $\theta_a \equiv E/RT_\infty$;

The nondimensional vaporisation rate is $\lambda = \dot{m}/(4\pi a_0 k_\infty/c_p)$ and the nondimensional droplet radius, $a = a/a_0$. According to d^2 law, the ratio λ/a, known as vaporisation constant and defined as β, depends on the heat flux to the droplet imposed by the flame and is a constant value.

The soot formation mechanism is idealised by a infinite fast reaction, given by a first order reaction, $F \rightarrow Soot$, at the position $x = x_{so}$,

$$\dot{\omega}_{so} \sim \lambda_{so}\delta(x - x_{so}) \tag{4}$$

In this idealised model, the values of λ_{so} and x_{so} are known. The value of λ_{so} must satisfy the following condition: $\lambda_{so}/\lambda = \phi/S$ with $\phi = O(1)$.

The form of the soot chemical reaction, Eq. (4), imposes a discontinuity in the first derivative of the fuel mass fraction and temperature. The jump conditions at the soot formation zone, $x = x_{so}$, are

$$\left[\frac{x^2\theta^n}{\lambda} \frac{\partial}{\partial x} \left\{ \frac{Sy_F}{(1+S)\theta/Q} \right\} \right]_{x_{so}^-}^{x_{so}^+} = \left\{ \begin{array}{c} 1 \\ \phi_q\bar{S} \end{array} \right\} SLe_F \int_{x_{so}^-}^{x_{so}^+} \dot{\omega}_{so}x^2 dx \tag{5}$$

in which $\phi_q \equiv (Q_{so}/Q)$ and $\bar{S} \equiv (1+S)/S$.

Equations (2) are integrated from the droplet surface $x = $ a to the ambient atmosphere $x \to \infty$, the flame is at a position between these two boundaries. To proceed the integration, the boundaries conditions must be specified; at $x = $ a $\equiv a/a_0$:

$$-\frac{x^2\theta^n}{Le_F} \frac{\partial y_F}{\partial x} = \lambda(1 - y_{Fs}), \quad x^2\theta^n \frac{\partial \theta}{\partial x} = \lambda l + q^- = \lambda l',$$

$$\theta = \theta_s, \quad y_F = y_{Fs} = exp[\gamma(1 - \theta_b/\theta_s)] \tag{6}$$

and for $x \to \infty$:

$$\theta - 1 = y_O - 1 = y_F = 0 \tag{7}$$

The subscript s represents the droplet surface condition. The nondimensional latent heat l is expressed by $L/(c_pT_\infty)$, q^- is the heat to inside the droplet. The parameter γ is defined as $\gamma = L/RT_b$.

In this work, it is admitted uniform temperature profile inside the droplet and close to the boiling value, $\theta = \theta_s < \theta_b$. Thereby, the mass conservation equation for the liquid phase leads to

$$\frac{d\text{a}^2}{d\tau} = -2\frac{\lambda}{\text{a}} \tag{8}$$

The closure for the system of equations is provided by the dimensionless equation of state of the gas, $\varrho\theta = 1$.

The system of Eqs. (1) and (2) is characterised by the boundary conditions Eqs. (6) and (7).

According to the type of the problem, at the flame $x = x_p$, the properties are

$$\theta - \theta_p = y_F - y_{Fp} = y_0 - y_{Op} = 0 \tag{9}$$

Equation (9) expresses the droplet problem in a general form, either fuel and oxygen leak by the flame. Under reactants leakage condition, the flow field analysis does not provide a closed solution. The flame properties (position and temperature of the flame) and the droplet properties (droplet temperature and vaporisation rate) are determined as function of the fuel leakage quantity. For these conditions, the Shvab-Zeldovich formulation with the excess enthalpy $H \equiv (1+S)\theta/Q + y_F + y_O$ and the mixture fraction $Z \equiv Sy_F - y_O + 1$ (Fachini, 1999),

$$\frac{\lambda}{x^2} \frac{\partial H}{\partial x} - \frac{1}{x^2} \left(x^2\theta^n \frac{\partial H}{\partial x} \right) + \left\{ \begin{array}{l} [(Le_F - 1)/S] (\lambda/x^2) \partial Sy_F/\partial x \quad + \\ \\ (1 - Le_O)(\lambda/x^2)\partial(-y_O)/\partial x \end{array} \right\} =$$

$$-[1 + (1 + S)\phi_q]SLe_F\dot{\omega}_{so} \tag{10}$$

$$\frac{\lambda}{x^2}\frac{\partial Z}{\partial x} - \frac{1}{x^2}\left(x^2\theta^n\frac{\partial Z}{\partial x}\right) + \left\{\begin{array}{ll}(Le_F - 1)(\lambda/x^2)\partial Sy_F/\partial x & + \\ \\ (Le_O - 1)(\lambda/x^2)\partial(-y_O)/\partial x & \end{array}\right\} = -SLe_F\dot{\omega}_{so} \tag{11}$$

is not able to solve the problem in a closed form. To determine the solution in a close form is necessary to integrate the species conservation equations together with Eqs. (10) and (11).

The three characteristic parameters for the soot modelling, ϕ, ϕ_q and x_{so}, define, respectively, mass of soot, heat required and the position of the soot formation zone relatively to the flame position. They will be changed in order to verify the extension of the model and the influence on the soot formation in the droplet combustion properties. Naturally, three finger-controlled parameters are an excessive number of parameters for a simple model. In fact, a model with three finger-controlled parameters is able to describe even a "elephant".

The equations for H and Z satisfy the boundary conditions at the droplet surface $x = $ a, which are determined from Eq. (3),

$$H_s \equiv H(\mathrm{a}) = (1 + S)\,\theta_s/Q + y_{Fs}, \qquad Z_s \equiv Z(\mathrm{a}) = Sy_{Fs} + 1, \tag{12}$$

$$F_H \equiv \frac{x^2\theta^n}{\lambda}\left.\frac{\partial H}{\partial x}\right|_{x=\mathrm{a}} = (1 + S)\,l'/Q - Le_F(1 - y_{Fs}), $$

$$F_Z \equiv \frac{x^2\theta^n}{\lambda}\left.\frac{\partial Z}{\partial x}\right|_{x=\mathrm{a}} = -SLe_F(1 - y_{Fs}) \tag{13}$$

at the flame $x = x_p$, the boundary conditions are given from Eq. (4),

$$H(x_p) = (1 + S)\theta_p/Q + y_{Fp} + y_{Op}, \qquad Z(x_p) = Sy_{Fp} - y_{Op} + 1, \tag{14}$$

and from the ambient atmosphere $x \to \infty$

$$H(\infty) = (1 + S)/Q + 1, \qquad Z(\infty) = 0, \tag{15}$$

It is admitted that all soot particle, after being formed, is pushed to the droplet but does not hit the surface. The soot particle finds a position where the drag force is equal to the thermophoretic force. In this preliminary analysis, the soot shell and its effects are not included in the model. Thus, the soot formation will act only on the reduction of the flame temperature and of the flame position.

3. BURKE-SCHUMANN KINETIC

Burke-Schumann kinetic mechanism considers the reactions infinitely fast, thereby by the flame there is no leakage of reactants. The following condition is satisfied $y_F.y_O = 0$, or $y_{Fp} = y_{Op} = 0$ at the flame. Under this condition, the flame takes place where the fuel flux meets the oxidant flux in stoichiometric proportion and the position is defined as $x = x_p = x_f$.

Thereby, by imposing no leakage condition, Eqs. (10) and (11) simplify to (Fachini, 1999; Fachini et al., 1999),

$$\frac{\lambda}{x^2}\frac{\partial}{\partial x}\left(H + \int_{Z_s}^{Z} N(Z)dZ\right) - \frac{1}{x^2}\frac{\partial}{\partial x}\left(x^2\theta^n\frac{\partial H}{\partial x}\right) = -\left(\frac{1+\phi_q}{S} + \phi_q\right)SLe_F\dot{\omega}_{so} \quad (16)$$

$$\frac{\lambda}{x^2}\frac{\partial}{\partial x}\int_{Z_s}^{Z} L(Z)dZ - \frac{1}{x^2}\frac{\partial}{\partial x}\left(x^2\theta^n\frac{\partial Z}{\partial x}\right) = -SLe_F\dot{\omega}_{so} \quad (17)$$

where

$$N(Z) = \begin{cases} (Le_F - 1)/S, & Z > 1 \\ (1 - Le_O), & Z < 1 \end{cases}, \qquad L(Z) = \begin{cases} Le_F, & Z > 1 \\ Le_O, & Z < 1 \end{cases}$$

From the definition of the functions H and Z, the original variables are defined as following:

$$\theta = \begin{cases} [H - (Z-1)/S]\, Q/(1+S), & Z > 1 \\ [H + (Z-1)]\, Q/(1+S), & Z < 1 \end{cases}, \qquad \begin{array}{l} y_F = (Z-1)/S, \quad Z > 1 \\ y_O = (1-Z), \qquad Z < 1 \end{array}$$

The jump condition for the first derivative of H and Z functions represents the soot formation and it is determined integrating the Eqs. (16) and (17) around $x = x_{so}$. This procedure leads to the following expressions

$$\left[\frac{x^2\theta^n}{\lambda}\frac{\partial H}{\partial x}\right]_{x_{so}^-}^{x_{so}^+} = \left(\frac{1+\phi_q}{S} + \phi_q\right)\frac{SLe_F}{\lambda}\int_{x_{so}^-}^{x_{so}^+}\dot{\omega}_{so}x^2dx$$

$$\left[\frac{x^2\theta^n}{\lambda}\frac{\partial Z}{\partial x}\right]_{x_{so}^-}^{x_{so}^+} = \frac{SLe_F}{\lambda}\int_{x_{so}^-}^{x_{so}^+}\dot{\omega}_{so}x^2dx \quad (18)$$

By integrating Eqs. (16) and (17) from the droplet surface up to a position x,

$$H - H_s + F_H + \int_{Z_s}^{Z} N(Z)dZ - \frac{x^2\theta^n}{\lambda}\frac{\partial H}{\partial x} = -\left(\frac{1+\phi_q}{S} + \phi_q\right)\frac{SLe_F}{\lambda}\int_a^x \dot{\omega}_{so}x^2dx \quad (19)$$

$$\int_{Z_s}^{Z} Le(Z)dZ + F_Z - \frac{x^2\theta^n}{\lambda}\frac{\partial Z}{\partial x} = -\frac{SLe_F}{\lambda}\int_a^x \dot{\omega}_{so}x^2dx \quad (20)$$

The value of F_H and F_Z are given by Eq. (13).

As seen in previous works, the function H can be expressed as a function of the mixture fraction Z as following

$$\frac{dH}{dZ} = \frac{H - H_s + F_H + \int_{Z_s}^{Z} N(Z)dZ + [(1+\phi_q)/S + \phi_q](SLe_F/\lambda)\int_a^x \dot{\omega}_{so}x^2dx}{\int_{Z_s}^{Z} Le(Z)dZ + F_Z + (SLe_F/\lambda)\int_a^x \dot{\omega}_{so}x^2dx} \quad (21)$$

From Eq. (17), the mixture fraction Z is a function of the position, $Z = Z(x)$. From Eqs. (12), (13) and (15), the behaviour of Z can be studied. Since $Z_s > Z(\infty)$ and $\partial Z/\partial x|_a < 0$, then Z decreases monotonically and $x = x(Z)$ is found.

From Eq. (4), $\dot{\omega}_{so} \sim (\lambda/S)\delta(x - x_{so})$, the soot reaction terms in Eq. (21) can be represented by the following expression

$$\frac{S}{\lambda} \int_a^x \dot{\omega}_{so} x^2 dx = \phi_m \int_{Z_s}^Z \delta(Z - Z_{so})dZ \tag{22}$$

Recalling, the values for ϕ_m, ϕ_q and Z_{so} are known. For convenience, instead of ϕ, ϕ_m is used. From Eq. (4), ϕ_m and ϕ are related according to $\phi_m = \phi x_{so}^2$.

Instead of working with ϕ, it was more convenient to use the combination $\phi_m = \phi x_{so}^2$.

Note that, by increasing Z_{so}, the soot reaction zone takes place far from the flame, it means a decrease in x_{so}. Thus, for a fixed value of ϕ_m, any increase in the soot formation makes the soot reaction zone to be close to the droplet; it means Z_{so} becomes larger.

The solution of Eq. (21) permits to determine the temperature at the droplet surface θ_s ($Z = Z_s$), the eigenvalue of the excess enthalpy equation and, as part of the solution, the flame temperature θ_f ($Z = 1$). After the integration of Eq. (21), the integration of Eq. (20) may be performed because the boundary condition at the droplet surface is determined by Eq. (6); $Z_s \equiv S y_{Fs}(\theta_s) + 1$. As seen from Eqs. (12), (13) and (15), there is an extra condition to be imposed to the solution of Eq. (20). The extra condition leads to determining the eigenvalue $\lambda = \lambda(n, Le_F, Le_O, \phi_q, \phi_m, Z_{so})$. The flame position $x = x_f$ is also found as part of the solution of Eq. (20) imposing $Z(x_f) = 1$. Once knowing $H = H(Z)$, the variables $\theta = \theta(Z)$, $y_F = y_F(Z)$ and $y_O = y_O(Z)$ are found. Finally, after knowing $Z = Z(x)$, then $H = H(x)$, $\theta = \theta(x)$, $y_F = y_f(x)$ and $y_O = y_O(x)$ are found.

4. RESULTS AND COMMENTS

The results for the droplet combustion problem considering soot formation correspond to the n-heptane in an ambient temperature of $300K$. The properties for n-heptane are: heat of combustion $q = 4.4647 \times 10^6 J/mol$, latent heat $L = 4.2619 \times 10^4 J/mol$, boiling temperature $T_b = 371K$, ambient oxidant mass fraction $Y_{O\infty} = 0.21$, massic stoichiometric coefficient $\nu = 3.52$, fuel Lewis number $Le_F = 1.88$ and oxidant Lewis number $Le_O = 1.07$. In this model the isobaric specific heat c_p is considered constant, whose value is chosen $80 J/K.mol$. Besides c_p, the model has three more parameters to control the soot formation: modified soot formation rate, heat consumption and soot zone position represented by ϕ_m, ϕ_q and Z_{so}.

The solution of Eq. (21) is shown in Fig. 1a. As seen clearly, the soot formation makes the excess enthalpy profile H decreases. Another results from this solution are the determination of the droplet surface temperature θ_s and the flame temperature θ_f (Lima et al., 2006). The values for θ_s and θ_f will be depicted ahead. It is worth to mention that these two temperatures are not dependent directly on the transport coefficients, in other words the velocities of heat and mass transports, but on their ratios represented by the Lewis numbers.

After determining the droplet surface temperature θ_s, it is possible to find the fuel mass fraction y_{Fs} at the droplet surface via Eq. (6), the Clayperon relation. Thus, knowing y_{Fs}, the value for the mixture fraction Z_s at the droplet surface is specified, which is one of the boundary conditions needed to the integration of Eq. (20). The integration of Eq. (20) provides the dependence of the mixture fraction Z on the spatial coordinate x/a, $Z = Z(x)$, as seen in Fig. 1b. As occurred with the integration of Eq. (21), the integration of Eq. (20) provides the value of the ratio of the vaporisation rate λ to the droplet radius a(τ), $\beta = \lambda/a$, the eigenvalue of Eq. (20).

From $H = H(Z)$ and $Z = Z(x)$, the gas temperature θ and the fuel and oxidant mass fractions y_F and y_O, respectively, are determined. The temperature θ profile is exhibited in Fig. 1c and the fuel and oxidant mass fractions y_F and y_O are shown in Fig. 1d. In these four plots,
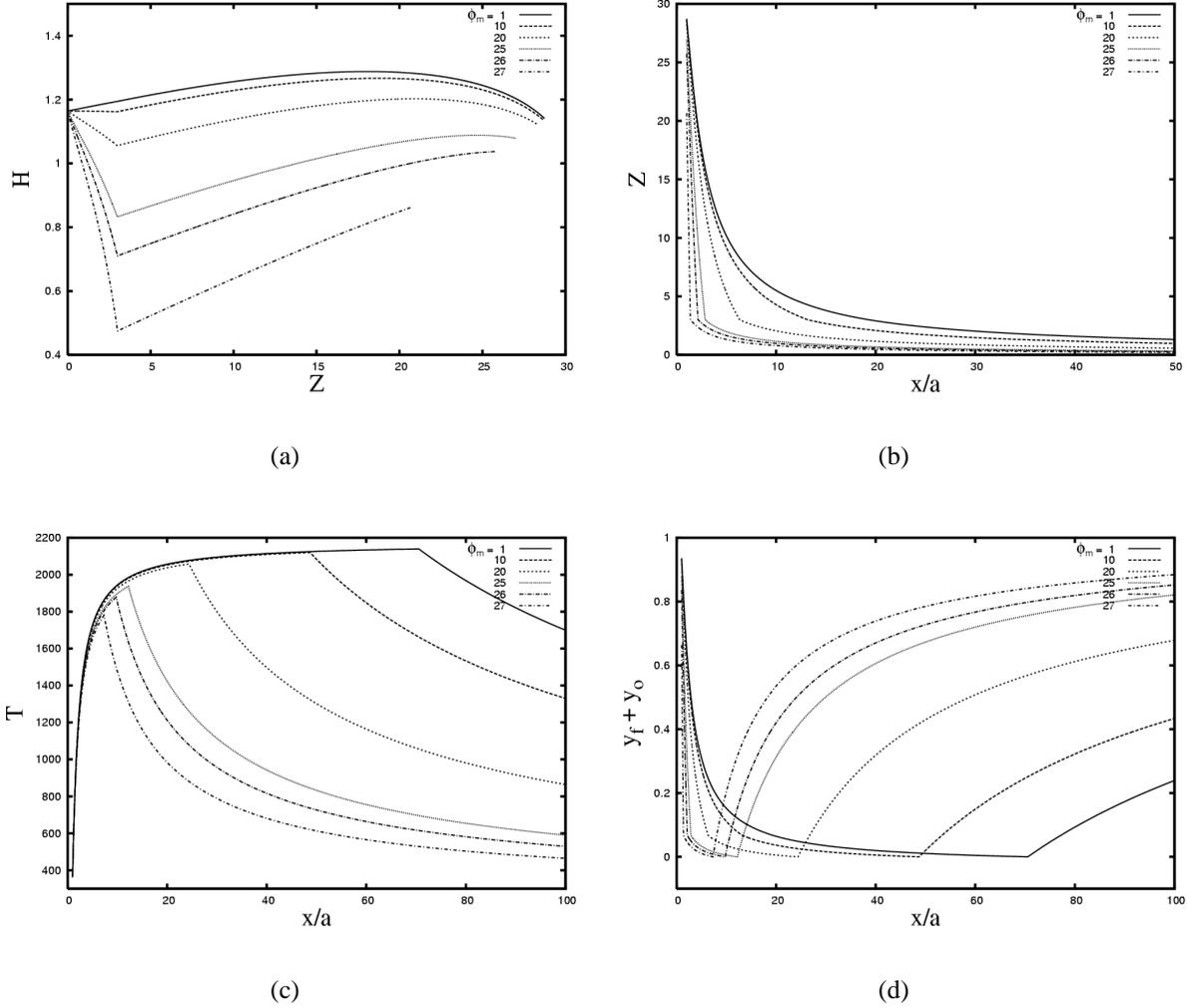
Figure 1: (a) The excess enthalpy H as function of the mixture fraction Z. (b) The mixture fraction Z as a function of the spatial coordinate x/a. (c) The temperature profile T as a function of the spatial coordinate x/a. (d) The fuel and oxidant mass fractions y_F and y_O as a function of the spatial coordinate x/a. These results were found for $\phi_q = 0$, $Z_{so} = 3$ and $1 \leq \phi_m \leq 27$.

the influence of the soot on the droplet combustion can be seen. As conditions favour formation of soot, the flame establishes closer to the droplet and the flame temperature reduces.

The soot model has three parameters, ϕ_m, ϕ_q and Z_{so}. To show their influence on the droplet combustion, ϕ_m is varied from 0 to 27 and meanwhile the other two parameters take values $Z_{so} = 1$, 1.25, 2, 3 and $\phi_q = 0$, 0.1, 0.2

4.1 Influence of ϕ_m and Z_{so}

In Fig. 2, the properties at the droplet surface are exhibited, H_s, Z_s, T_s/T_b and y_{Fs}, as a function of modified soot quantity ϕ_m and position of the soot zone Z_{so}. For $\phi_m < 20$, those properties almost do not change. Since H_s and Z_s do not change significantly, the boundary conditions for Eqs. (20) and (21) keep the same; recalling that the value for H_∞ and Z_∞ are fixed. Under these conditions, T_s and $\beta = \lambda/a$, the eigenvalues of Eqs. (20) and (21), do not vary significantly.

Recalling, the classical model is able to predict the experimental results concerning to the vaporisation rate, but it is not able to predict the temperature and position of the flame.

The discrepancy on the temperature and on the position is due to the infinity fast chemical reaction hypothesis (complete fuel consumption). To avoid this rigid hypothesis, a model with three degrees of freedom is showing to be able to reproduce experimental results for droplet combustion.
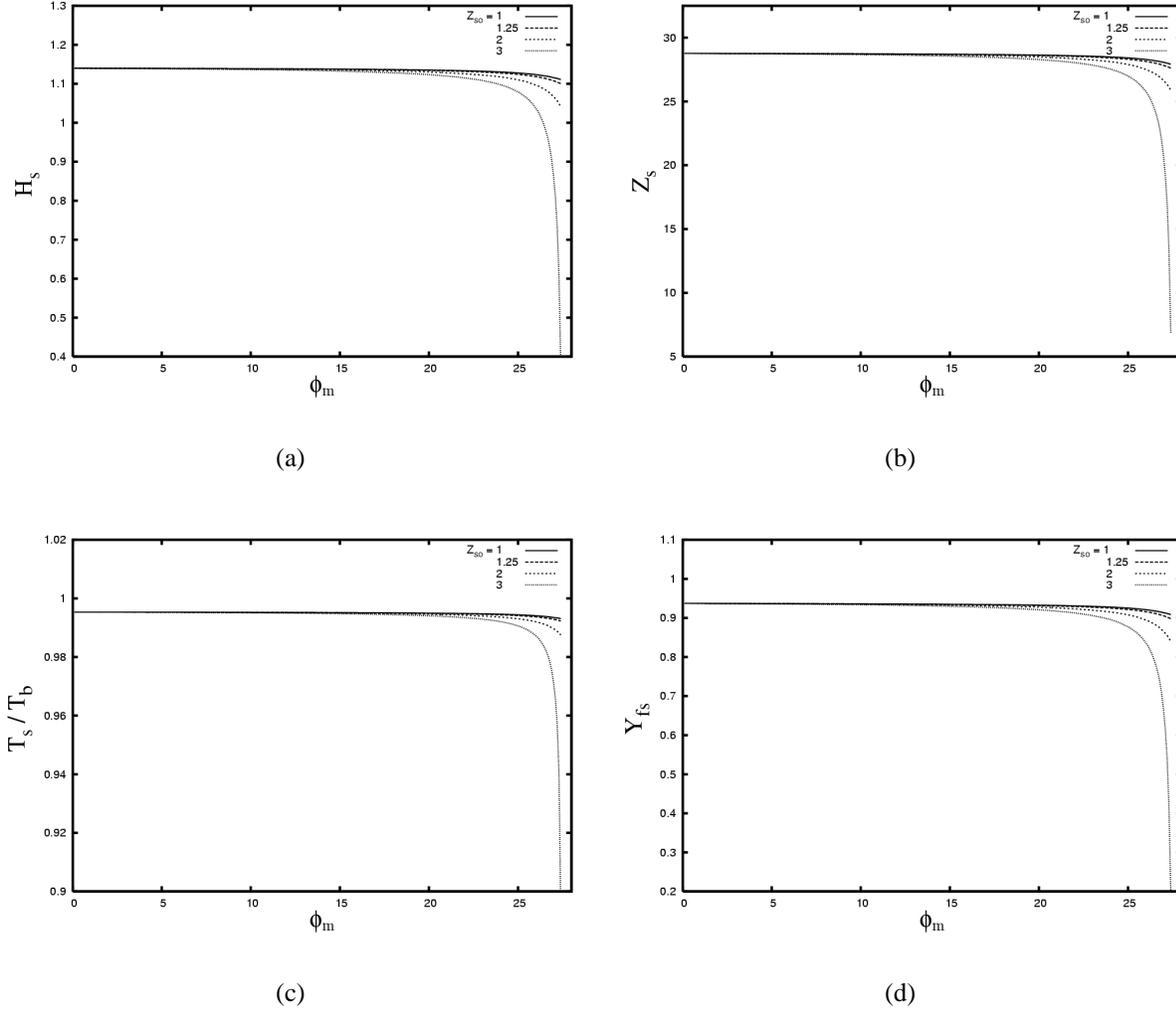

(a)

(b)

(c)

(d)

Figure 2: (a) Droplet surface excess enthalpy H_s as a function of the ϕ_m . (b) Droplet surface mixture fraction Z_s as a function of the ϕ_m. (c) Droplet surface temperature T_s/T_b as a function of the ϕ_m. (d) Droplet surface fuel mass fraction y_{Fs} as a function of the ϕ_m. These results were found for four values of the soot zone position $Z_{so} = 1$, 1.25, 2, 3; $\phi_q = 0$.

For $\phi_m > 20$, those properties start changing with ϕ_m and show to be sensitive to the location of the soot zone. As farther the soot zone is from the flame, that occurs increasing Z_{so}, as larger the effect of the soot is. The case $Z_{so} = 3$ reveals that the combustion can not be sustained for ϕ_m close to 27.4 because $\phi \sim S$, almost all fuel vapour is converted to soot. The consequence of this condition is: low flame temperature and low droplet surface temperature. Since the latent heat is high, low droplet surface temperature θ_s makes the fuel mass fraction y_{Fs} at the droplet surface to go to zero, i.e. no vaporisation. Note that the model considered conditions such that $\phi = O(1)$, so that results for $\phi \sim S$ is out of the model extension.

Figure 3 exposures the influence of the soot formation rate and the position of soot zone on the flame properties, temperature θ_f and position x_f. First of all, the position of the soot zone Z_{so} does not affect the flame properties. Also, the quantity of soot ϕ_m do reduce drastically the
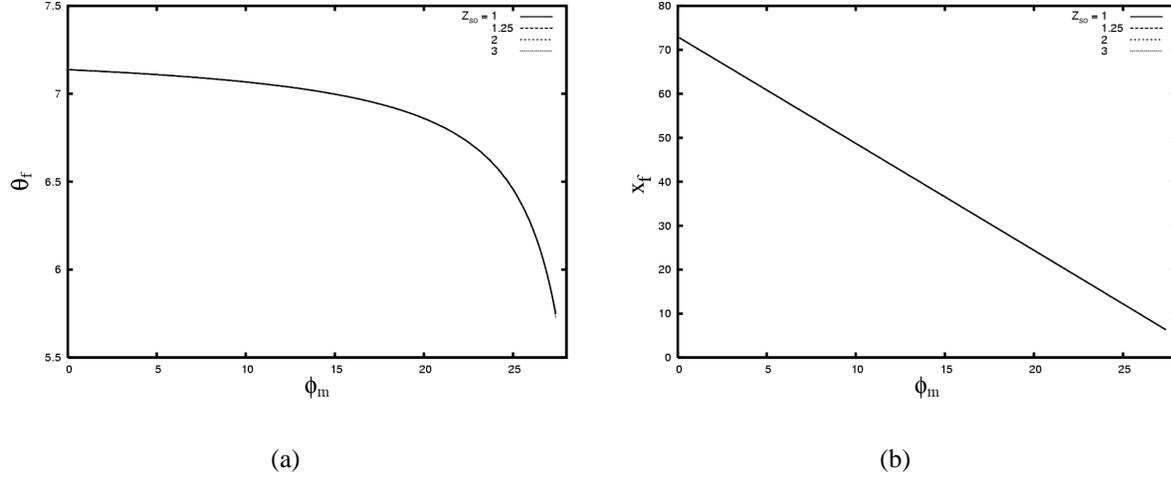
(a)

(b)

Figure 3: (a) Flame temperature θ_f as a function of ϕ_m. (b) Flame position x_f as a function of ϕ_m. These results were found for four values of the soot zone position $Z_{so} = 1,\ 1.25,\ 2,\ 3$; $\phi_q = 0$.

flame temperature and the flame position. Large ϕ_m means large soot formation, less fuel in the gas phase, small fuel flux to the flame and low flame temperature. An unexpected result was the linear decrease of the flame position x_f with ϕ_m.

Although the model neglects some processes, results from Figs. 2 and 3 are pointing that soot formation, even without considering the heat loss on the process $\phi_q = 0$, can be an explanation for the discrepancy between the experimental and classic theoretical results. Besides that the model considering soot formation provides vaporisation constant β that vary only slightly for $\phi_q = 0$, as seeing in in Fig. 4a. Note that β does not change with the location of the soot
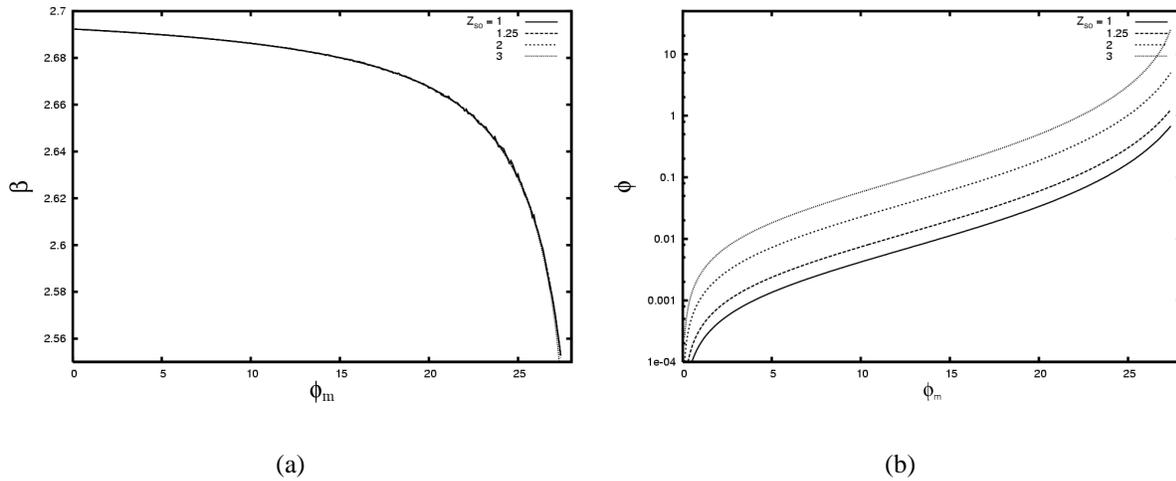

(a)

(b)

Figure 4: a) Vaporization constant β as a function of ϕ_m. b) Soot mass ϕ as a function of ϕ_m. These results were found for four values of the soot zone position $Z_{so} = 1,\ 1.25,\ 2,\ 3$; $\phi_q = 0$.

zone.

In Fig. 4b, the quantity of soot $\phi\ (\equiv \phi_m/x_{so}^2)$ is depicted. The combustion limit on $\phi_m = 27.4$ for the condition $\phi_q = 0$ and $Z_{so} = 3$ represents the soot formation rate almost equal to the vaporisation rate $\lambda_{so} \sim \lambda\ (\phi \sim S)$.

From the results depicted up to now, it is possible to say that, the inclusion of the soot formation is able to change drastically on the flame properties but is able to keep vaporisation

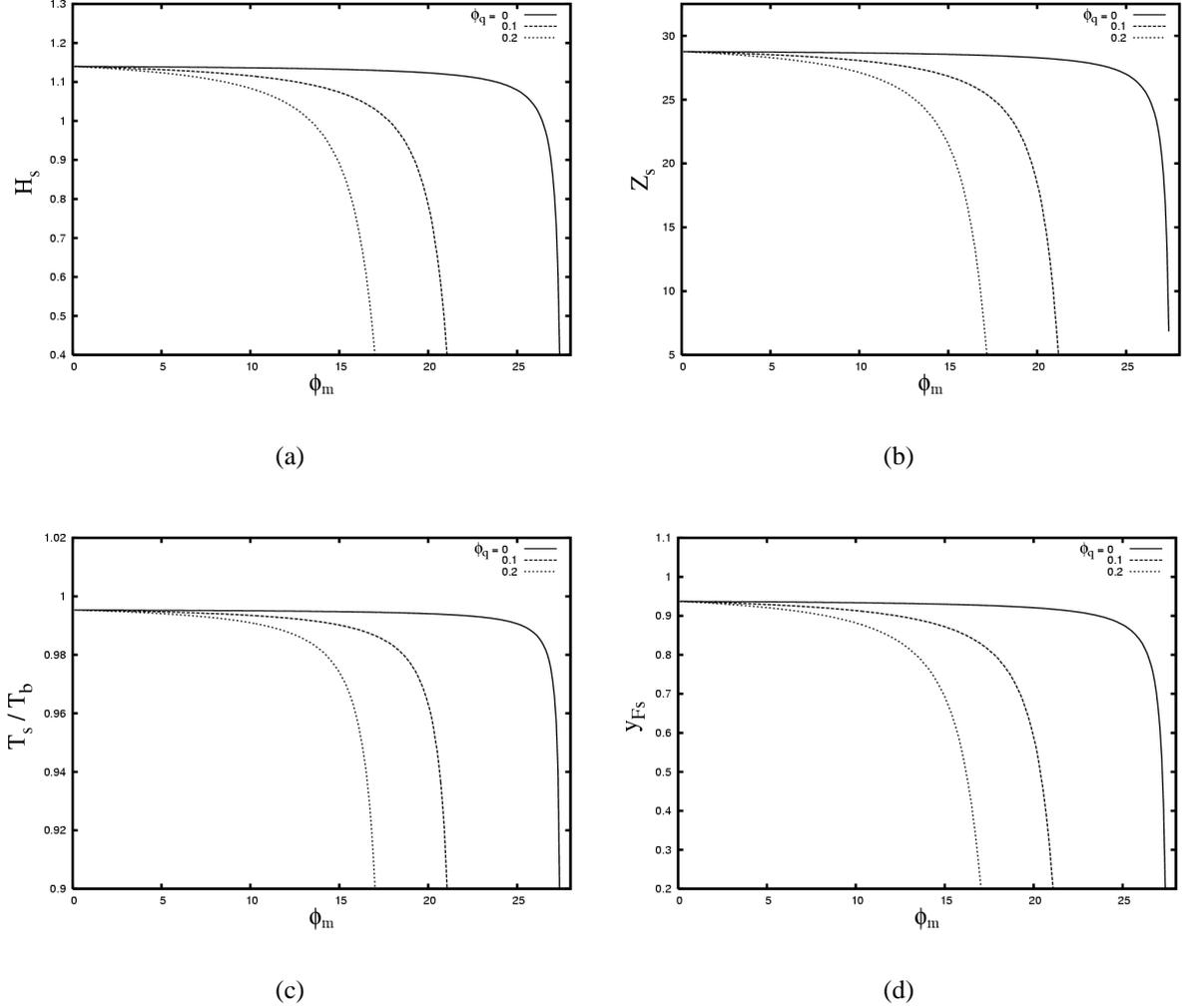constant with values close to the case without soot.

4.2 Influence of ϕ_m and ϕ_q

(a)

(b)

(c)

(d)

Figure 5: (a) Droplet surface excess enthalpy H_s as function of ϕ_m. (b) Droplet surface mixture fraction Z_s as a function of ϕ_m. (c) Droplet surface temperature T_s/T_b as a function of ϕ_m. (d) Droplet surface fuel mass fraction y_{Fs} as a function of ϕ_q. These results were found for $\phi_q = 0,\ 0.1,\ 0.2$ and $Z_{so} = 3$.

Results in Fig. 5 depict clearly limit for the droplet combustion. The quantity of soot is such that imposes a strong reduction on the droplet surface temperature and consequently on the droplet surface fuel mass fraction y_{Fs}. These conditions impose a very weak combustion regime because $\phi \sim S$, out of the focus of this analysis. The extinction can not be observed because the model assumes infinite fast reaction, however the weak combustion regime is an indication of no sustainable burning conditions.

Plots 5a and 5b show the value of the excess enthalpy H_s and mixture fraction Z_s at the droplet surface. Since H_s and Z_s are the boundary conditions of Eqs. (20) and (21), reduction in their values represent a decrease in the problem eigenvalues, θ_s (represented as T_s/T_b) and $\beta = \lambda/a$. The behaviour of the droplet surface temperature T_s/T_b and the droplet surface fuel mass fraction y_{Fs} are seen in plots 5c and 5d, respectively.

The inclusion of the soot formation heat $\phi_q > 0$ is responsible to strong reduction in the flame temperature θ_f, as seen in plot 6a. The results seen in plot 6b show a small deviation of

the linear decreasing behaviour of the flame position x_f with ϕ_m, thus the linear behaviour is still a good approximation.

The strong reduction on droplet combustion properties has a direct reflection on the vaporisation rate represented by the vaporisation constant β. Figure 7a shows an important reduction on the vaporisation constant β as a function of the soot formation heat ϕ_q.

The results pointed that the heat loss on the soot formation process is responsible to strong variation of the vaporisation constant β. Moreover, the limit explicitly presented in previous figures represent the weak combustion regime when $\phi \gg 1$, as observed in Fig. 7b.

5. CONCLUSION

A simplified soot model is incorporated in the droplet combustion model. The soot is supposed to be formed totally in a infinite thin zone, not distributed in a region with high temperature. The results showed that the soot formation is a good explanation for the discrepancy between classic theoretical results to experimental results. An unexpected result was the linear deacrese of the flame position x_f with the modified soot formation rate ϕ_m for the cases $\phi_q = 0$ and a good approximation for $\phi_q > 0$. Heat loss is important for the determination of the vaporisation constant β.

This analysis can be used as a very low cost numerical tool to determine the droplet condition in combustion spray codes.
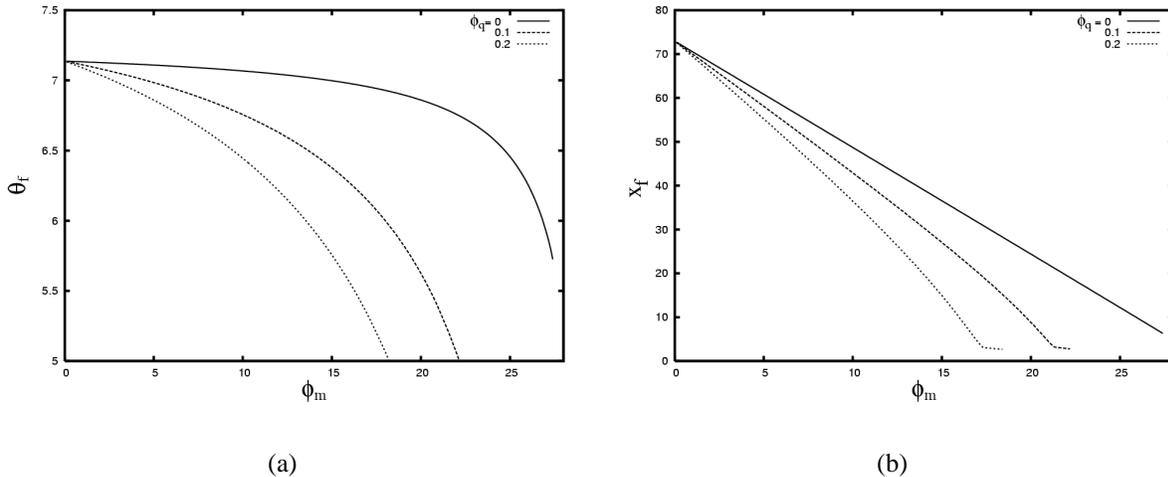

(a)   (b)

Figure 6: (a) Flame temperature θ_f as a function of ϕ_q. (b) Flame position x_f as a function of ϕ_m. These results were found for $\phi_q = 0$, 0.1, 0.2 and $Z_{so} = 3$

REFERENCES

Akerman, M., Hicks, M., Nayagam, V., Williams, F. A., 2005. Combustion of droplets in steady and unsteady slow flows in microgravity. 43rd AIAA Aerospace Sciences Meeting and Exhibit, AIAA paper 2005–1139, Reno NV, Jan. 10–13.

Avedisian, C. T., 2000. Recent advances in soot formation from spherical droplet flames at atmospheric pressue. J. Prop. Power 16, 628–635.
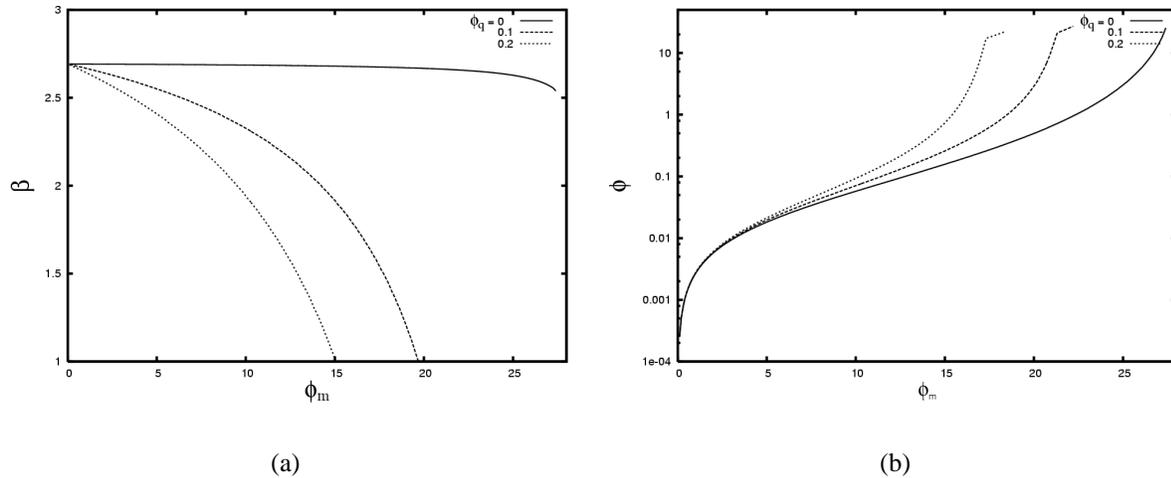
Figure 7: Vaporization constant β as a function of ϕ_m. These results were found for four values of the soot zone position $\phi_q = 0,\ 0.1,\ 0.2;\ Z_{so} = 3$.

Avedisian, C. T., Jackson, G. S., 2000. Soot patterns around suspended n-heptane droplet flames in a convection-free environment. J. Prop. Power 16, 974–979.

Fachini, F. F., 1999. An analytical solution for the quasi-steady droplet combustion. Combust. Flame 116, 302–306.

Fachini, F. F., 2005. Quasi-steady droplet combustion with fuel leakage. 18th Brazilian Congress of Mechanical Engineering, COBEM2005, Paper 0738, Ouro Preto, MG, Nov. 6th to 11th, pp 1–9.

Fachini, F. F., Liñán, A., Williams, F. A., 1999. Theory of flame histories in droplet combustion at small stoichiometric fuel-air ratios. AIAA Journal 37, 1426–1435.

Faeth, G. M., 1977. Current status of droplet and liquid combustion. Prog. Energy Combust. Sci. 3, 191–224.

Kumar, S., Ray, A., Kale, S. R., 2002. A soot model for transient, spherically symmetric n-heptante droplet combustion. Combust. Sci. Techn. 174, 67–102.

Lima, L. E. M., Gonçalves, E. A., Moura, G. S., Fachini, F. F., 2006. Uma generalização da formulação de shvab-zel'dovich para combustão de gotas. 11th Brazilina Congress of Thermal Engineering and Sciences, ENCIT2006, Under Consideration, Curitiba, PR, iro, RJ, Dec. 5 to 8th, pp 1–5,.

Manzello, S. L., Yozgatligil, A., Choi, M. Y., 2004. An experimental investigation of sootshell formation in microgravity droplet combustion. Int. J. Heat Mass Transfer 47, 5381–5385.

Nayagan, V., Jr, J. B. H., Colantonio, R. O., Marchese, A. J., Dryer, F. L., Zhang, B. L., Williams, F. A., 1998. Microgravity n-heptane droplet combusiton in oxygen-helium mixtures at atmospheric pressure. AIAA Journal 36, 1369–1378.

Ueda, T., Imamura, O., Okay, K., Tsue, M., Kono, M., Sato, J., 2002. Combustion behavior of single droplets for sooting and non-sooting fuels in direct current electirc fields under microgravity. Proc. Combust. Instit. 29, 2595–2601.

Xu, G., Ikegami, M., Honma, S., Ikeda, K., nad P. M. Struk, D. L. D., 2004. Sooting characteristics of isolated droplet burning in heated ambient under microgravity. Int. J. Heat Mass Transfer 47, 5807–5821.